Separation Science and Technology
Publication details, including instructions for authors and subscription information:
http://www.informaworld.com/smpp/title~content=t713708471

Effect of Internal Coagulant on Morphology of Polysulfone Hollow Fiber Membranes. I

Jianshuo Yan; Wayne. W. Y. Lau

To cite this Article Yan, Jianshuo and Lau, Wayne. W. Y.(1998) 'Effect of Internal Coagulant on Morphology of Polysulfone Hollow Fiber Membranes. I', Separation Science and Technology, 33: 1, 33 — 55
To link to this Article: DOI: 10.1080/01496399808544754
URL: http://dx.doi.org/10.1080/01496399808544754

SEPARATION SCIENCE AND TECHNOLOGY, 33(1), pp. 33–55, 1998

Effect of Internal Coagulant on Morphology of Polysulfone Hollow Fiber Membranes. I

JIANSHUO YAN and WAYNE W. Y. LAU*
DEPARTMENT OF CHEMICAL ENGINEERING
NATIONAL UNIVERSITY OF SINGAPORE
REPUBLIC OF SINGAPORE 119260

ABSTRACT

Membrane separation performance is governed by membrane morphology. It is generally accepted that structure of the membrane skin layer is responsible for membrane selectivity while membrane flux depends on the total transmembrane resistance to material flow. In this study, polysulfone ultrafiltration hollow fiber membranes were made using the "dry-wet" fiber spinning process through a tube-in-orifice spinnerette. By using water as the external coagulant and a very short air gap, fibers with a dense outer skin layer were prepared which showed high selectivity in the separation of polyethylene glycols of various molecular weight. By using a mixture of water and 1-methyl-2-pyrrolidone in various proportions as the internal coagulant, demixing rates of the polymer in the spinning solution could be adjusted to yield a more open surface structure in the fiber inner surface layer and a more porous sublayer in the fiber wall to reduce the total transmembrane resistance. The rate of polymer demixing can be related to the difference between the solubility parameter of the internal coagulant and that of the polymer. This difference can serve as a scale to indicate the coagulation power of the internal coagulant. At low coagulation power, fibers with a more open structure in the fiber wall and its inner surface could be made which yielded higher membrane flux due to the lower transmembrane resistance in these fibers.

INTRODUCTION

From the standpoint of engineering, for a membrane to give high performance demands, in general, that the membrane must have high selectivity

* To whom correspondence should be addressed.

(or high rejection) and high membrane flux. In terms of membrane morphology, this demand translates to the requirements that the membrane must have the desired pore size in the skin layer and low resistance to material transfer across the membrane wall. The aim of the present study is to develop polysulfone ultrafiltration hollow fiber membranes of low transmembrane resistance with a selective skin layer on the fiber outer surface. In the conventional method of making hollow fiber through a spinnerette, water is often used as the internal coagulant in the fiber bore, and thus a dense skin layer is formed on the bore-side surface of the fiber. During ultrafiltration operation for such inner-skinned hollow fibers, the feed mixture is introduced through the fiber bore. In such separation operations there exists a limit to the applied pressure on the feed because a high applied pressure may cause the fiber to burst. On the other hand, when a feed mixture is introduced onto the outer surface of a hollow fiber, the fiber can withstand a much higher applied pressure to give a higher driving force for material transport across the membrane wall; that is, membrane flux is expected to increase in response to the higher applied pressure. Transmembrane resistance can be reduced when resistance at the fiber bore side is low. Fibers of low bore-side resistance can be made by using an internal coagulant other than pure water. By using an internal coagulant of low coagulation power, pores made at the fiber bore surface will be more open, thus helping to reduce the overall transmembrane resistance to mass flow across the membrane wall.

In this work, outer-skinned hollow fiber membranes with a highly porous inner surface and sublayer were spun through a spinnerette. The spinning solution consisted of polysulfone (PSF), 1-methyl-2-pyrrolidone (NMP, solvent), and polyvinylpyrrolidone (PVP, additive). A mixture of NMP and water in various proportions was used as the internal coagulant. The coagulation power of the internal coagulant was thus adjusted by varying the NMP/water proportions.

THEORETICAL BACKGROUND

Two types of phase separation processes are responsible for the formation of an asymmetric membrane (1, 2): gelation (or crystallization) for the formation of a dense skin, and liquid–liquid demixing for the formation of the porous sublayer.

Skin Formation

The formation of a skin layer is by gelation (for amorphous polymer) or crystallization (for a semicrystalline polymer). At a high polymer con-

centration the molecular chains entangle and interact more intensively with each other when the polymer used has a molecular weight greater than its critical molecular weight for entanglement. The more numerous the entanglements, the more dense and viscous the gel will be. When entanglements and interactions reach a certain degree, movement of the polymer chains are highly restricted and thus a membrane skin is formed. Due to the high viscosity of this skin layer, the interdiffusion rates of solvent and nonsolvent are so low that liquid–liquid demixing by nucleation and growth is suppressed. A dense skin is thus formed. This process is favored by a lower ratio of nonsolvent/solvent interchange.

Sublayer Formation

According to Reuvers et al. (3), two types of delayed demixing can be distinguished, one where the nonsolvent/solvent ratio interchange is low, resulting in densification of the top layer, where porous or nonporous top layers may be formed. The other type is where the outflow of solvent is relatively low or even negative, as when the solvent concentration in the coagulation bath is higher than in the polymer solution, so that demixing occurs at lower polymer concentrations as will happen when solvent is added to the nonsolvent coagulant. The region of highly concentrated polymer solution just beneath the cast film surface increases until the onset of liquid–liquid demixing. So a thick intermediate layer just beneath the skin can be distinguished. Because the polymer concentration in this layer is relatively high at the moment of onset of liquid–liquid demixing, the porosity and interconnectivity of cavities will be relatively low. Beneath this significantly dense intermediate layer is the highly porous sublayer. The initial polymer concentration in this layer hardly increases until the onset of liquid–liquid demixing in this layer, so the transmembrane resistance of this kind of membrane is mainly determined by the dense skin layer and the intermediate layer. The thickness of this skin layer is an important factor for material transport.

Instantaneous demixing is a process in which liquid–liquid demixing happens as soon as the cast film contacts the coagulation medium. Nuclei of the diluted phase are formed just beneath the top layer where the initial polymer concentration has hardly changed. The induced porosity and interconnectivity of cavities will be relatively high, so the transmembrane resistance of this kind of membranes is mainly determined by the dense skin layer. The thickness of this dense skin is an important factor for membrane transport. This type of membranes typically consist of a very thin dense skin layer on a microporous sublayer connected to a support layer of open cell fingerlike voids or sponge.

Influence of Coagulation Medium

The influence of solvent in the coagulation medium (e.g., water) had been investigated by many workers (3–11). It was found that the addition of solvent into the coagulation medium decreased its coagulation power. Thus, during membrane immersion precipitation, the ratio of the counterflow rate of solvent and nonsolvent is decreased and a delayed demixing results. For a ternary polymer solution, composition paths for different initial solvent concentrations in the coagulation medium were calculated by Reuvers (3). Polymer concentration at the interfacial boundary of the film will decrease if the initial solvent concentration in the coagulation medium is increased. As a result, the membrane skin thickness decreases and a uniform pore structure across the membrane thickness is formed. If the initial solvent concentration in the coagulant is high enough, the interfacial boundary between the cast film and the coagulation medium will disappear. The polymer at the interface begins to dissolve in the coagulant and a microporous surface is formed.

Solubility Parameter

The concept of solubility parameter was developed to describe the enthalpy of mixing of simple liquids (nonpolar, nonassociating solvents). Although it has been extended to polar solvents and polymers, it does not give consistent results when used for polar systems. The solubility parameter was developed from *regular solution* theory by Hildebrand. By his definition, "a regular solution is one involving no entropy change when a small amount of one of its components is transferred to it from an ideal solution of the same composition, the total volume remaining unchanged" (12). In other words, a solution described as "regular" is one which, despite a nonideal (nonzero, either positive or negative) enthalpy of formation, has an ideal entropy of formation. This can occur only if random distribution of molecules persists even in the presence of component i and component j where i–j interactions differ from the original i–i and j–j interactions. The concept has proved valuable in the development of an understanding of miscibility criteria and of deviations from ideality. Unfortunately, although the term "regular solution" has come into general use, the usage does not always conform with its original definition.

Because an amorphous polymer such as PSF is "liquidlike" in some of its properties, its solubility behaviors can be treated by methods used for a regular solution if allowances are made for the differences due to one of the components being made up of very long molecules and the other of small molecules. Thermodynamically, the process of dissolving an amorphous polymer in a solvent is governed by

$$\Delta G_m = \Delta H_m - T\Delta S_m \tag{1}$$

where ΔG_m is Gibbs energy change of mixing, ΔH_m is enthalpy change of mixing, T is absolute temperature, and ΔS_m is entropy change on mixing. A negative ΔG_m predicts that the mixing process will occur spontaneously.

According to the Flory–Huggins lattice theory, the entropy of mixing of polymer and solvent ΔS_m can be expressed as

$$\Delta S_m = -R(x_1 \ln \phi_1 + x_2 \ln \phi_2) \tag{2}$$

where x_i is the mole fraction of component i, ϕ_i is the volume fraction of component i, and R is the ideal gas constant. Since $\phi_i < 1$ and $\ln \phi_i < 0$, ΔS_m is always positive. The dissolution of a high-molecular-weight polymer always leads to a large increase in entropy, thus the enthalpy term (the sign and the magnitude of ΔH_m) is the deciding factor in determining the sign of the Gibbs energy change. ΔH_m is given by

$$\Delta H_m = \Delta E_m + P\Delta V \tag{3}$$

where ΔE_m is the cohesive energy of mixing, P is the system pressure, and ΔV is the volume change during mixing. Since there is no volume change on mixing in regular solutions, then Eq. (3) can be written as

$$\Delta H_m = \Delta E_m \tag{4}$$

The cohesive energy of mixing ΔE_m can be expressed as

$$\Delta E_m = (x_1 V_1 + x_2 V_2) A_{12} \phi_1 \phi_2 \tag{5}$$

where V_i is the molar volume of component i, A_{12} is the *exchange energy density* or *exchange cohesive pressure* given by

$$A_{12} = c_1 + c_2 - 2c_{12} \tag{6}$$

c_i in Eq. (6) is the *cohesive energy density* (cohesive energy per unit volume) of component i, $c_i = -E_i/V_i$. The solubility parameter δ is defined as the square root of the cohesive energy density:

$$\delta_i = c_i^{0.5} = \left(-\frac{E_i}{V_i}\right)^{0.5} \approx \left(\frac{\Delta E_i^V}{V_i}\right)^{0.5} \tag{7}$$

where ΔE_i^V is the energy of vaporization of component i.

c_{12} in Eq. (6) is the cohesive pressure characteristic of the intermolecular forces acting between molecules of Components 1 and 2. For a regular solution the geometric mean approximation can be used:

$$c_{12} = (c_1 c_2)^{0.5} \tag{8}$$

so

$$A_{12} = (c_1^{0.5} - c_2^{0.5})^2 = (\delta_1 - \delta_2)^2 \tag{9}$$

Thus ΔH_m can be written as

$$\Delta H_m = \Delta E_m = (x_1 V_1 + x_2 V_2)[\delta_1 - \delta_2]^2 \phi_1 \phi_2 \tag{10}$$

and ΔG_m becomes

$$\Delta G_m = (x_1 V_1 + x_2 V_2)[\delta_1 - \delta_2]^2 \phi_1 \phi_2 + RT(x_1 \ln \phi_1 + x_2 \ln \phi_2) \tag{11}$$

Binodal curves and spinodal curves can be calculated from this equation, and thus the behavior of polymer demixing can be predicted. The thermodynamics of phase separation in polymer is thus described in term of the solubility parameter difference $(\delta_1 - \delta_2)$. In order for ΔG_m to be less than zero, the heat of mixing must be smaller than the entropic term. ΔG_m will always be less than zero for regular solutions when $\delta_1 = \delta_2$, which indicates that the components will be miscible in all proportions. In general $(\delta_1 - \delta_2)^2$ must be small for Component 1 and Component 2 to be miscible.

The solubility parameter of a two-component mixture can be calculated using (13)

$$\delta = \phi_1 \delta_1 + \phi_2 \delta_2 \tag{12}$$

where ϕ_1 and ϕ_2 are volume fractions of the components. The solubility parameter difference $\Delta\delta$ for a coagulant and a polymer in solution can be calculated using

$$\Delta\delta = |\delta_c - \delta_p| \tag{13}$$

where δ_c and δ_p are the solubility parameters of the coagulant and the polymer in solution, respectively. The larger is $\Delta\delta$, the larger will be ΔG_m, and thus the less miscible will be the polymer with the coagulant. Thus $\Delta\delta$ serves as a scale of coagulation power of the coagulant. A higher coagulation power of the coagulant will cause faster demixing (precipitation) of the polymer from its solution. In the following sections, $\Delta\delta$ of the internal coagulant used for making hollow fibers will be correlated to fiber morphology and thus fiber performance.

EXPERIMENTAL

Materials

Polysulfone (PSF, Udel 3500) was obtained from Amoco, water-soluble polyvinylpyrrolidone (PVP, MW = 10,000, additive) was obtained from

Sigma, 1-methyl-2-pyrrolidone (NMP, solvent) was obtained from Merck, and polyethylene glycols (PEG) of molecular weights from 2k to 35k, used as molecular probes, were supplied by Aldrich and Merck. The solubility parameter δ of PSF is 21.5 $MPa^{0.5}$ (14), δ of PVP is 25.6 $MPa^{0.5}$ (14), δ of NMP is 23.1 $MPa^{0.5}$, and δ of water is 47.9 $MPa^{0.5}$ (15).

Demixing Kinetics

Liquid–liquid demixing rate of a polymer solution can be monitored by light transmission experiments. When an incident beam of light travels through a flat cast polymer solution film in contact with a coagulant, the faster is the reduction of intensity of transmitted light by the film due to polymer precipitation, the higher is the demixing rate and vice versa. The experimental setup used for the light transmission studies is schematically shown in Fig. 1. When an initially thermodynamically stable and transparent cast film on a glass plate contacts the coagulant in the bath, diffusion-induced phase separation can be observed in the films as indicated by optical inhomogeneities that cause light transmittance to decrease with time. Light transmitted through the cast film was measured by a digital light meter. A relative light transmittance, RLT, is defined herein as

$$RLT = (LT - LT_{min})/(LT_{max} - LT_{min}) \quad (14)$$

where LT_{max} is the maximum light transmission through the polymer solution film at time 0, LT_{min} is the minimum light transmission through the film at the end of an experiment, and LT is the light transmission at time t. In these experiments, coagulants of the same NMP/water compositions used as the internal coagulant in fiber spinning were used as the coagulation medium for these light transmission experiments.

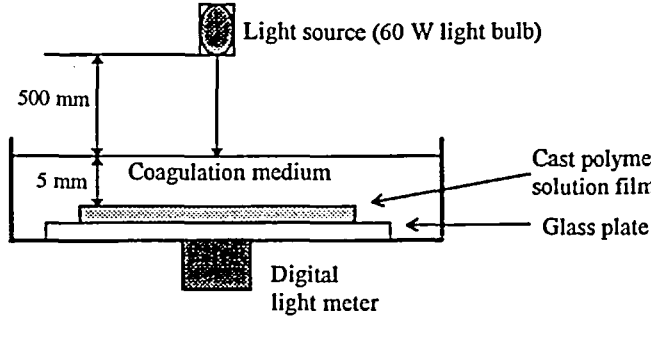

FIG. 1 Experimental set-up for light transmission experiments.

Fiber Spinning Solution

Spinning solutions of different compositions and viscosity (Table 1) were prepared as follows: PSF was dried at 150°C for 3 hours before use. Measured quantities of PSF, PVP, and NMP were mixed in a glass bottle. The bottle was placed on a roll-mixer to mix for 3 hours every day and kept in an oven at 60°C every night. When a transparent, homogeneous solution was obtained, fibers were spun using a procedure reported elsewhere (16). In this study, NMP/water mixtures of various compositions were used as the internal coagulant and water alone was used as the external coagulant, and the air gap was kept small (less than 1 cm). Afterward the fiber was cut into lengths of 60–70 cm and rinsed in another water bath for 3 days to leach out residual solvent and additive from the fiber.

Scanning Electron Microscopy

Scanning electron microscopy (SEM) was used to study the macroscopic structure and microscopic structure of the hollow fiber membranes. Low magnification was used for measurement of fiber outer diameter (OD), fiber inner diameter (ID), shape of the fiber cross-section, and fiber wall thickness from SEM micrographs. Higher magnification was used for measurement of fiber skin layer thickness, pore size, size of nodules at the fiber inner surface, and voids in the fiber cross-section.

Membrane samples for SEM were prepared by breaking the fiber samples at liquid nitrogen temperature. The broken samples were coated with a thin gold layer by sputtering. A Jeol JSM-T330A and a Hitachi Model 4100 scanning electronic microscopes were used. Porosity [(pore area)/(fiber surface area)] of the fiber surface can be calculated when the pores on the fiber surface can be seen from the micrograph.

TABLE 1
Compositions of the Spinning Solutions

	Solution code							
	11	12	13	16	18	19	20	22
PSF (wt%)	24	24	29	24	22	22	20	18
PVP (wt%)	10	15	10	20	10	15	10	10
PSF + PVP (wt%)	34	39	39	44	32	37	30	28
Viscosity (cP)	8,494	25,625	23,936	45,056	4,224	10,137	2,208	1,109

Ultrafiltration

Ultrafiltration (UF) performance data of the fibers in terms of solute rejection and membrane flux were collected. In this work, hollow fiber modules for UF were fabricated in the configuration of a shell-and-tube heat exchanger. Four to 10 fibers (depending on the fiber OD), in length 29 cm, were assembled into a bundle and inserted into a 1/2-inch diameter stainless steel tube. The bundle ends were potted using epoxy glue but the fiber bores were left open. After curing the epoxy for 5 hours, the hollow fiber bundle was ready for testing. Before testing, the shell-side of the module was filled with air under pressure to check for leakage. The feed mixture to the module was 200 ppm PEG in water. The feed mixture was introduced to the shell-side and to the tube-side to investigate performance difference between the outer surface and inner surface of the hollow fibers. The feed mixture was pumped by a centrifugal pump at 21 psi, and the feed flow rate was kept at 1.25 L/min for all UF tests. Under such test conditions the PEG concentration in the feed solution was kept low and the feed flow rate was kept high so that concentration polarization was assumed negligible. Permeate samples were collected at atmospheric pressure and weighed, and their PEG concentrations were analyzed using a Shimadzu Total Carbon Analyzer Model 5000. Thus the membrane separation factor f ($= 1 - C_p/C_f$) can be calculated, where C_p is solute concentration in the permeate and C_f is solute concentration in the feed. Pure water was also used as feed before and after the PEG test to obtain PWP (pure water permeation) data.

Membrane resistance and fouling resistance can be calculated from Darcy's law:

$$J_v = (\Delta P - \Delta\Pi)/\eta(R_m + R_f) \tag{15}$$

where J_v = flux (m/s)
ΔP = transmembrane pressure drop (Pa)
$\Delta\Pi$ = osmostic pressure of solutes (Pa)
η = viscosity (Pa·s)
R_m = membrane resistance (m^{-1})
R_f = fouling resistance (m^{-1})

RESULTS AND DISCUSSION

Effects of PSF Concentration

In a homogeneous, well-dispersed polymer solution, linear polymer (such as PSF) molecules occupy their own domain in solution space and the polymer–polymer interaction is weak. When the polymer chain length

is longer than a critical value, polymer–polymer entanglement is possible when the polymer concentration in the solution is increased. Polymer entanglements begin at a critical polymer concentration. The critical number of main chain atoms Z_c for strong polymer–polymer entanglement is 600 (17). Z of commercially available PSF is about 3000 [estimated from polyethersulfone (18)]. As shown in Fig. 2, a critical PSF concentration C_{cr} appeared at about 22.5 wt%. Above this critical concentration, polymer–polymer entanglements are so intense that a small addition of polymer to the solution causes a large viscosity increase. This same critical polymer concentration was found by Wood et al. (18). Above this critical concentration, the mobility of the macromolecules is lowered considerably. Thus high viscosity of the spinning solution will retard the polymer precipitation rate during the phase inversion process. Besides, higher pressure has to be applied to a viscous spinning solution to extrude the solution from the spinnerette, and rheological effects such as die-swell will become more pronounced which would affect the fiber dimensions.

In UF operation, solute separation is mainly governed by the pore size in the fiber skin layer, which in turn is governed by local distribution of polymer molecules at the moment of polymer precipitation. When PSF concentration in the spinning solution is high, more polymer chains per unit volume are deposited in the membrane skin layer, resulting in a dense membrane. Thus a membrane produced from a spinning solution of high PSF concentration has a higher transmembrane resistance. PWP (pure

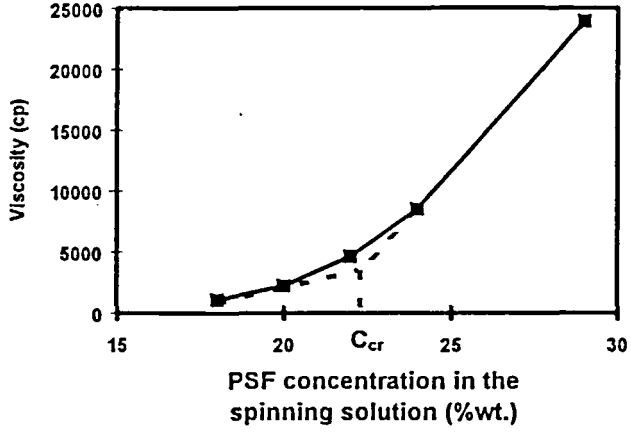

FIG. 2 Effect of PSF concentration in the spinning solution on viscosity. PVP concentration was kept at 10 wt%.

water permeation) through this membrane will be lower (Fig. 3a) and its solute separation will be correspondingly higher (Fig. 3b). It is interesting to note in Fig. 3(b) that the highest solute separation occurred with fibers made from a solution of 22 wt% PSF, very close to the estimated critical PSF concentration of 22.5 wt% PSF shown in Fig. 2. Above this PSF concentration, entanglement among PSF molecules can be expected to be very high, and dense membrane skin layers will be formed.

Polymer Precipitation Rate

Coagulation Power of the Coagulant

The rate at which a polymer can be precipitated from its solution by a coagulant depends on the coagulation power of the coagulant. As the coagulation power increases, the polymer–solvent interaction in the polymer solution is lowered. Thus the polymer precipitation rate increases in response to an increase in the coagulation power. The coagulation power of the coagulant can be reflected by the solubility parameter difference $\Delta\delta$ between δ_p of the polymer in solution and δ_c of the coagulant (19). As shown in Eq. (11), $\Delta\delta$ carries the significance of a thermodynamic property and can be used to predict the behavior of polymer phase separation. When $\Delta\delta$ is high, the coagulation power of the internal coagulant for the polymer is high and polymer demixing is thermodynamically possible (Eq. 11). The light transmission vs time curves obtained by immersing the cast films in coagulants with different $\Delta\delta$ are shown in Fig. 4, in which values of the initial slopes indicate demixing rates. The higher $\Delta\delta$ is, the faster

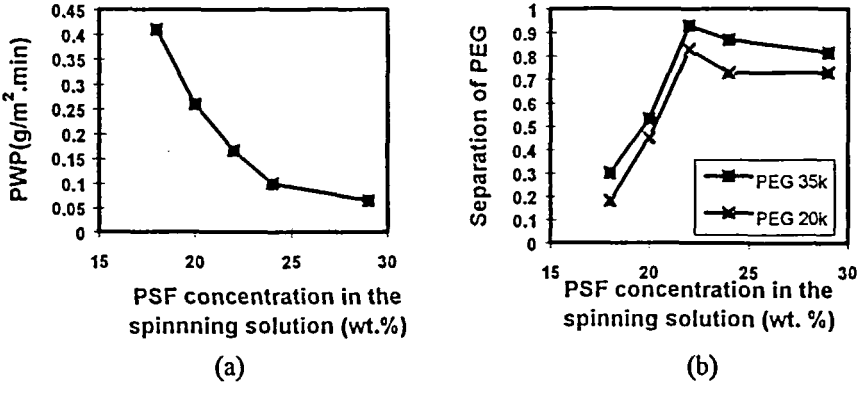

FIG. 3 Effect of PSF concentration in the spinning solution on (a) PWP and (b) PEG separation. PVP concentration was kept at 10 wt%. $\Delta\delta$ = 4.1 $MPa^{0.5}$. Shell-side feed.

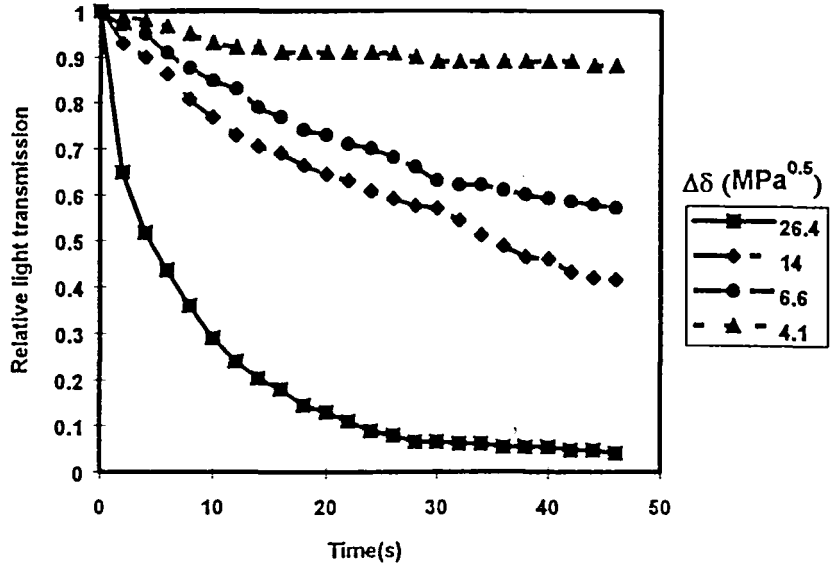

FIG. 4 Relative light transmission through cast film immersed in coagulant of different $\Delta\delta$s. Polymer solution: PSF/NMP/PVP = 24/66/10.

(potentially) will be the demixing rate of the polymer from solution. The PSF demixing rate was indeed dependent on $\Delta\delta$, as shown in Fig. 5. When $\Delta\delta$ was as large as 26.4 $MPa^{0.5}$, the transmitted light decreased very fast, indicating that instantaneous polymer demixing took place. When $\Delta\delta$ was of medium value (about 6–18 $MPa^{0.5}$), the initial slope values decreased, which can be considered to denote delayed demixing. When $\Delta\delta$ was as small as 4.1 $MPa^{0.5}$, the light transmission vs time curve showed a relatively flat profile, indicating that little or no polymer was precipitated.

It is also seen in Fig. 5 that the initial slope values of the light transmission vs time curve for a low PSF content solution are higher than those for a high PSF content solution. This was mainly due to the high viscosity of the polymer solution. Polymer demixing was severely hindered by the high viscosity and a low $\Delta\delta$. Boom et al. (9) and Radovanoic et al. (11) also found that the polymer precipitation rate decreased as the polymer content in the solution increased.

Viscosity of the Coagulant

It was found by several researchers (10, 20) that the viscosity of the coagulant is also an important factor influencing the polymer precipitation

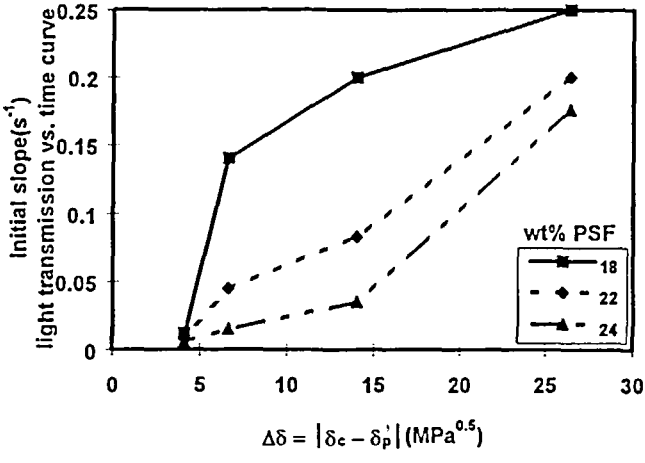

FIG. 5 Dependence of rate of demixing of PSF on $\Delta\delta$. PVP concentration was kept at 10 wt%.

rate and thus the membrane morphology. The viscosity of the coagulant causes changes in the kinetics of polymer precipitation. To study this effect, the viscosity of the coagulant was increased by the addition of different amounts of PVP (MW 10,000) in water. The compositions of the coagulants and their viscosities are listed in Table 2.

The light transmission vs time curves obtained by immersing the cast films in coagulants with different viscosities are shown in Fig. 6. The initial polymer precipitation rate decreased as the viscosity of the coagulant increased. At this time scale ($t < 20$ seconds), the high viscosity of the coagulant retarded the mass transfer rate between the polymer film and the coagulant, i.e., the solvent/nonsolvent counterdiffusion rate. But after a period when the concentration of nonsolvent diffusing into the polymer film reached a certain level, the polymer precipitation rate started to increase and reached the same rate as in a low viscosity environment. The high viscosity of the coagulant could only temporarily delay polymer phase separation. After a delayed period the polymer film could still be

TABLE 2
Compositions and Viscosity of the Coagulants Containing Water and PVP

PVP (wt%)	5	10	20	30	50	60	67 (saturated)
Viscosity (cP)	2	2.8	5	18	200	1,040	12,460

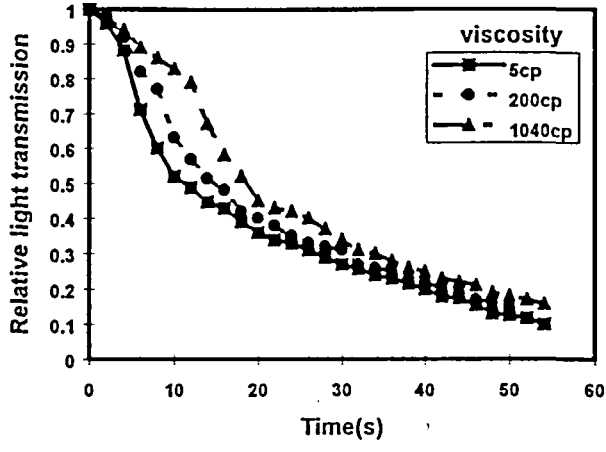

FIG. 6 Relative light transmission through nascent film immersed in coagulant of different viscosities. Polymer solution: PSF/NMP/PVP = 24/66/10.

precipitated by the coagulant, even when its viscosity was as high as 1040 cP. Only at very high viscosity (>5000 cP) of the coagulant could polymer precipitation be severely retarded (10). A coagulant of high viscosity is difficult to handle in a fiber spinning operation. It is very difficult to spin hollow fibers using an internal coagulant whose viscosity is higher than 1000 cP. For control of the polymer demixing rate at the fiber bore, varying the viscosity of the internal coagulant is not as effective as varying its $\Delta\delta$.

Effects of Internal Coagulant on Hollow Fiber Spinning

Hollow fibers were spun using the dry-wet spinning technique. During fiber spinning, the composition of the internal coagulant was varied by adding different amounts of solvent NMP to water to form a mixture which contained up to 90 wt% NMP. The solubility parameter δ of the internal coagulant corresponding to its composition was in the 47.9–25.6 $MPa^{0.5}$ range. Water alone was used as the external coagulant. The flow rate of the internal coagulant was controlled at 0.2–0.3 L/h.

Macroscopic Fiber Structure

It was found that the fiber dimensions were also dependent on the magnitude of $\Delta\delta$ when the flow rate of the internal coagulant was kept con-

stant. As shown in Fig. 7(a), the OD and ID of the hollow fiber decreased when $\Delta\delta$ decreased from 26.4 to 9 $MPa^{0.5}$. The nascent fiber was easier to stretch under gravitation when the fiber inner surface layer underwent delayed demixing. When $\Delta\delta$ decreased from 9 to 4.1 $MPa^{0.5}$, the fiber OD decreased due to gravitational pull on the nascent fiber but the fiber ID began to increase because the lateral expansion of the internal coagulant had a more pronounced effect on the nascent fiber than did gravitation. When $\Delta\delta$ was lower than 4.1 $MPa^{0.5}$, the internal coagulant began to penetrate into the fiber wall and the viscosity of the nascent hollow fiber became even smaller than the viscosity of the spinning solution. At this stage, lateral expansion of the internal coagulant influenced the dimensions of the fiber. Thus, OD and ID increased simultaneously.

It is also shown in Fig. 7(a) that the fiber wall thickness increased and reached a maximum as $\Delta\delta$ decreased. At high $\Delta\delta$ the nascent fiber was fixed immediately once it was extruded out of the spinnerette through a short air gap. The fiber wall thickness was thus not influenced by the physical forces. As $\Delta\delta$ decreased, the polymer precipitation rate decreased. The fiber wall thickness increased and reached a maximum at $\Delta\delta = 9$ $MPa^{0.5}$. At low $\Delta\delta$, the nascent fiber could not be precipitated before it entered the external water bath. In its nascent state other forces such as gravitation and expansion (under a hydrostatic head) of the internal coagulant stretched the nascent fiber longitudinally and laterally, and thus the fiber wall thickness decreased.

The above discussions are valid during spinning of a low viscosity solution. As shown in Fig. 7(b), a similar situation was found in the spinning solution of PSF/NMP/PVP = 20/70/10, where the maximum fiber wall thickness was found at $\Delta\delta = 6.6$ $MPa^{0.5}$, while for the spinning solution of PSF/NMP/PVP = 22/68/10, it was at $\Delta\delta = 9$ $MPa^{0.5}$ due to a lower PSF concentration in the former solution. A spinning solution with a low polymer concentration can be precipitated by an internal coagulant of medium coagulation power which cannot precipitate a solution of high polymer content. Upon polymer precipitation the nascent hollow fiber gained self-support from the precipitated polymer at the fiber inner surface layer to counteract the effect of gravitation. Thus the maximum fiber wall thickness shifted to occur at lower $\Delta\delta$. During the spinning of a high viscosity solution, such as PSF/NMP/PVP = 24/56/20, viscosity = 45,056 cP, the die-swell effect appeared to play a more important role at high $\Delta\delta$ than for spinning a solution of lower viscosity. As shown in Fig.7(c), the fiber wall thickness increased significantly as $\Delta\delta$ decreased from 26.4 $MPa^{0.5}$ and reached a maximum at $\Delta\delta = 9$ $MPa^{0.5}$. This die-swell effect was not so predominant at low $\Delta\delta$.

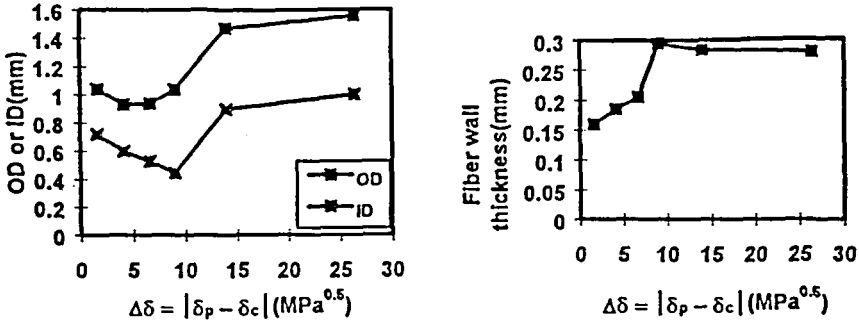

(a)

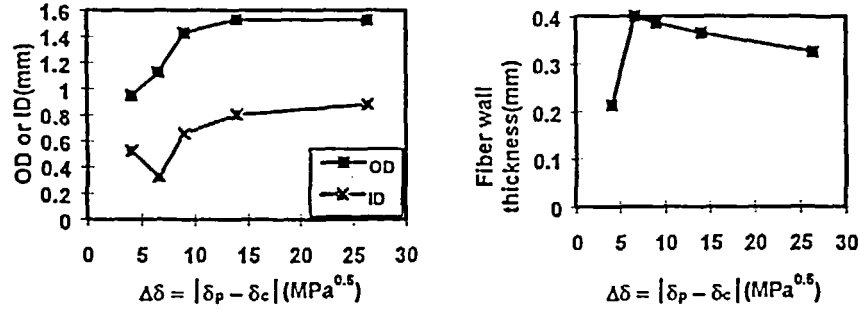

(b)

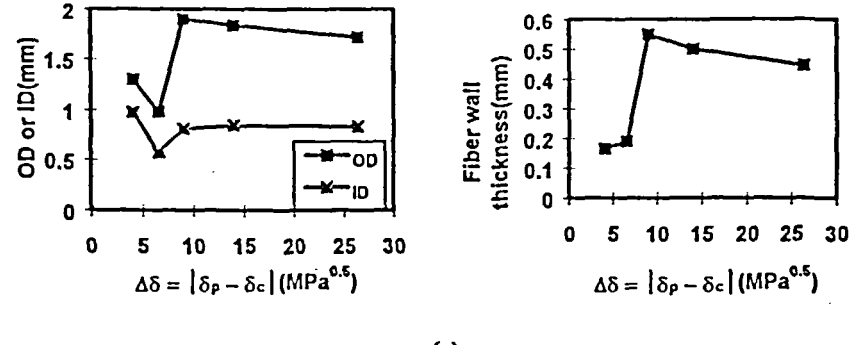

(c)

FIG. 7 Effect of $\Delta\delta$ on OD, ID, and fiber wall thickness of hollow fibers spun from different spinning solutions: (a) PSF/NMP/PVP = 22/68/10, (b) PSF/NMP/PVP = 20/70/10, (c) PSF/NMP/PVP = 24/56/20.

Microscopic Fiber Structure

When a small air gap (less than 1 cm) was used in the fiber spinning process, the morphology of the fiber outer skin layer was relatively independent of the composition of the internal coagulant. As soon as the extruded nascent fiber entered the external coagulation medium, instantaneous demixing took place on the fiber outer surface and the precipitation front advanced from the outside toward the inside of the nascent fiber. So in all experiments where a small air gap was used, a selective skin layer was formed on the fiber outer surface. Pores on the fiber outer surface were too small to be observed.

Skin layer formation at the bore side of the hollow fiber is influenced by the chemical nature of the internal coagulant (for example, its solubility parameter). The skin is formed by gelation of polymer particles (macromolecules or their aggregates). As pointed out by Strathmann (21), if skin formation occurs rapidly, particle growth in the skin will be kept to a minimum, and the skin will consist of coalesced fine particles, and therefore fine pores. If skin formation is delayed, particle growth continues, and particle and pore size increase. When water alone was used as the internal coagulant ($\Delta\delta = 26.4\ MPa^{0.5}$), instantaneous demixing took place, advancing from the nascent fiber inner surface toward its outer surface. The particle size and pore size in the fiber inner surface were very small, and a dense inner skin was formed on the fiber inner surface. Figure 8(a) shows this inner skin layer. The inner skin layer thickness was about 500 nm. Nodules of 20–45 nm in diameter were found packed tightly immediately under this inner skin. Since PSF is an amorphous polymer, this nodule formation was not caused by (partial) crystallization. Spinodal decomposition may be responsible for the formation of this nodular structure. These nodules varied in size, with the smallest near the fiber inner surface, increasing in size into the fiber wall, which gradually changed to a thick intermediate layer consisting of small open channels. These openings gradually increased in size, and a porous substructure could be seen. Macrovoids were formed in this porous substructure, and they grew deeper into the fiber wall. The size and number of macrovoids near the fiber inner surface were bigger than those near the fiber outer surface. Macrovoids mark the precipitation front of polymer demixing. The precipitation front from the fiber inner surface and that from the fiber outer surface met at some place in the fiber wall nearer the fiber outer surface. The biggest cavities across the fiber wall were found at this place in the fiber wall, and the smallest cavities were found in the skin layers.

Pores in the fiber inner surface were too small to be observed (Fig. 9a). When water alone was used as both the internal and external coagulant,

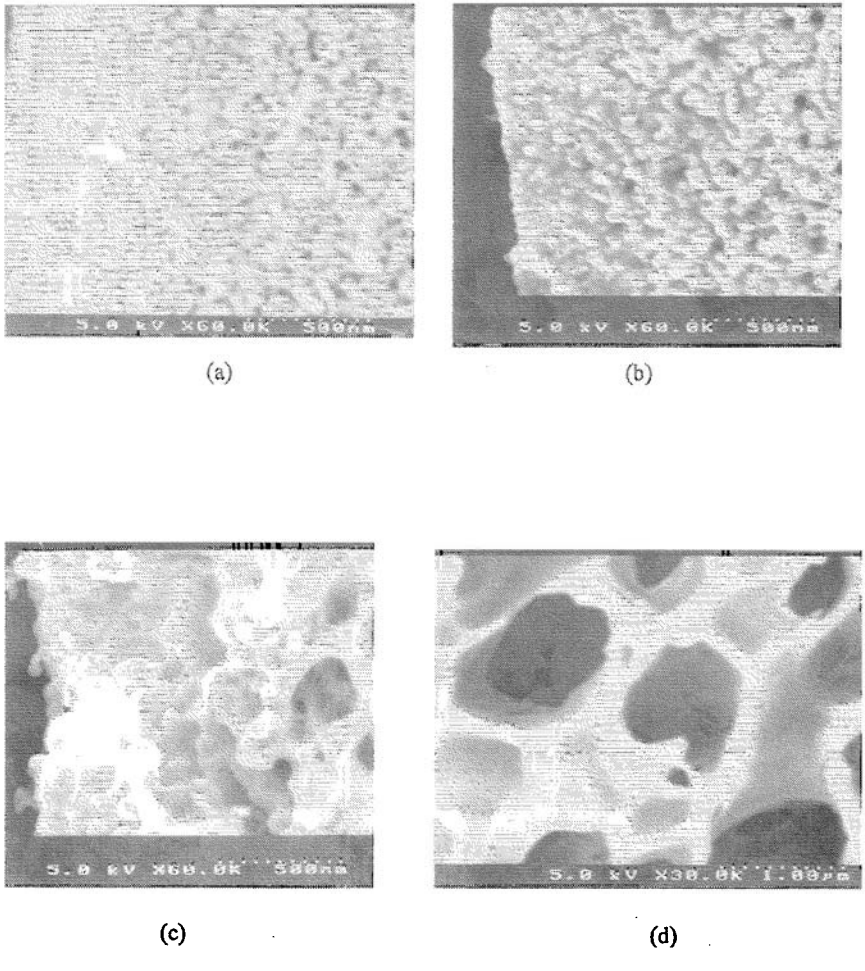

FIG. 8 The inner surface layer of hollow fiber spun from spinning solution PSF/NMP/PVP = 22/68/10, using (a) 0 wt% NMP in the internal coagulant, $\Delta\delta$ = 26.4 $MPa^{0.5}$; (b) 50 wt% NMP in the internal coagulant, $\Delta\delta$ = 14 $MPa^{0.5}$; (c) 80 wt% NMP in the internal coagulant, $\Delta\delta$ = 6.6 $MPa^{0.5}$; (d) 90 wt% NMP in the internal coagulant, $\Delta\delta$ = 4.1 $MPa^{0.5}$.

and the nascent fiber was spun through a small air gap, almost the same demixing mechanisms and demixing rates occurred at both fiber surfaces to yield a fiber whose inner skin layer structure and outer skin layer structure were similar.

Addition of a solvent (NMP) in the internal coagulant (water) results in a decrease in coagulation power of the internal coagulant, which induces

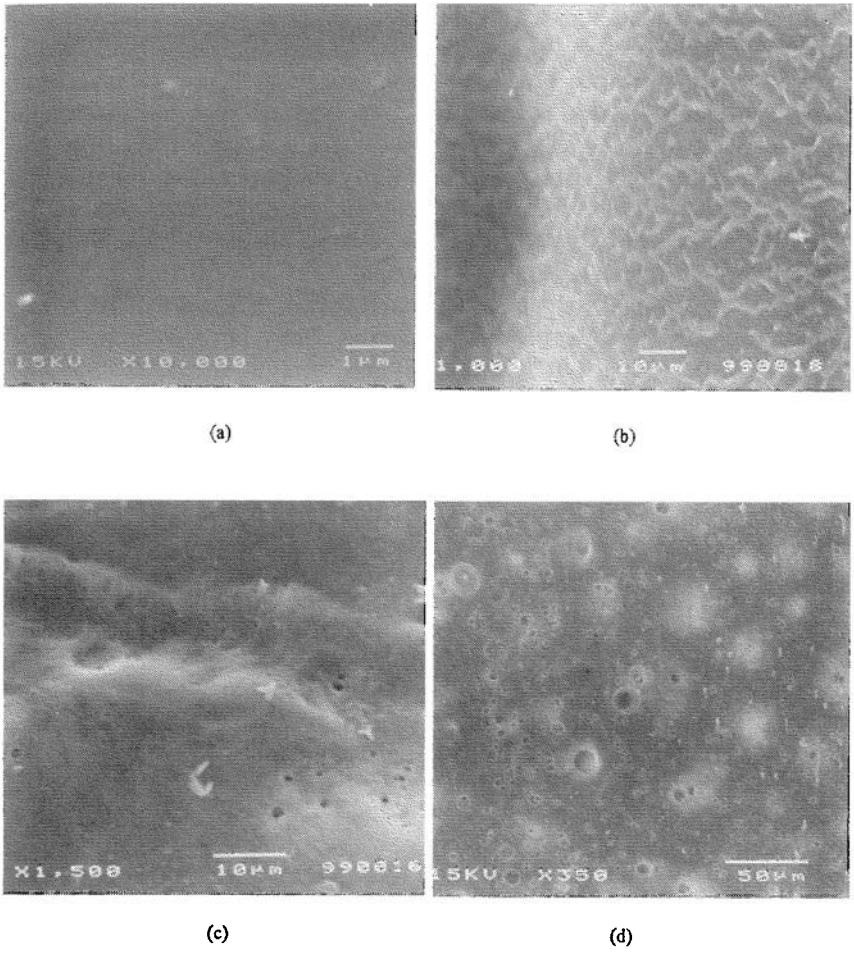

FIG. 9 Effect of $\Delta\delta$ on morphology of the fiber inner surface. Spinning solution: PSF/NMP/PVP = 22/68/10. (a) $\Delta\delta$ = 26.4 $MPa^{0.5}$, (b) $\Delta\delta$ = 14 $MPa^{0.5}$, (c) $\Delta\delta$ = 6.6 $MPa^{0.5}$, (d) $\Delta\delta$ = 4.1 $MPa^{0.5}$.

a slower polymer precipitation rate at the fiber bore side. When $\Delta\delta$ was decreased to 14 $MPa^{0.5}$, bigger nodules of about 54 nm in diameter could be seen packed loosely beneath the inner skin (Fig. 8b). The thickness of the intermediate layer was also reduced. The size and number of macrovoids originating from the fiber inner surface were smaller than those originating from the fiber outer surface. The biggest cavities across the

fiber wall were found nearer the fiber bore side rather than near the fiber outer surface when water alone was used as the internal coagulant, indicating that the polymer precipitation front, which started from the fiber inner surface, moved at a slower rate than one starting from the fiber outer surface. The two precipitation fronts met at a position in the fiber wall nearer the fiber inner surface. There were no observable pores on the fiber inner surface. The fiber inner skin surface appeared rougher (Fig. 9b) than one formed using water as the internal coagulant (Fig. 9a). This rough surface suggests that the fiber inner skin was formed as a result of complete fusion of surface nodules occurring during the membrane formation process; the bigger the nodules, the rougher the skin.

When the solvent (NMP) content in the internal coagulant was high enough ($\geq$80 wt%), $\Delta\delta$ became too low ($\leq$6.6 $MPa^{0.5}$) to cause polymer precipitation at the fiber bore side. As a result, no dense inner skin was formed in the fiber. Under such low $\Delta\delta$, nodules at the fiber inner surface could grow bigger and merge with each other. Pores were formed among the incompletely merged nodules (Fig. 8c). Similar observations were reported by Wienk et al. (10). Very few macrovoids were present near the fiber bore side. The biggest cavities across the fiber wall were found nearer the fiber bore side. As shown in Fig. 9(c), some pores ($\sim$1.7 μm in diameter) were present on the fiber inner surface.

When $\Delta\delta$ was about 4.1 $MPa^{0.5}$, polymer molecules at the fiber inner surface did not precipitate but dissolved into the internal coagulant. During fiber spinning using such an internal coagulant of low $\Delta\delta$, when the newly spun fibers were cut into pieces and rinsed in a water bath, it was observed that fluid coming out of the fiber bore turned cloudy due to precipitation of dissolved PSF in the internal coagulant. There was no nodular structure beneath the inner surface in these fibers. Instead, cavities of large size were found in the inner surface layer (Fig. 8d). The size of these cavities decreased toward the fiber outer surface. Polymer at the fiber inner surface was dissolved by the internal coagulant of low $\Delta\delta$, and the internal coagulant tended to penetrate into the nascent fiber. Thus PSF concentration at the fiber inner surface and substructure was reduced.

When the nascent hollow fiber entered the external coagulation medium, instantaneous demixing took place on the fiber outer surface and a dense outer skin was formed. As the precipitation front advanced further from the fiber outer surface, it met higher resistance which lowered its rate of advance. Consequently, bigger voids were formed near the fiber inner surface. Starting immediately under the fiber outer skin, the macrovoids extended across the fiber wall and opened up at the fiber inner surface. No macrovoids originating from the inner surface could be observed. As shown in Fig. 9(d), the fiber inner surface of this kind of fiber

was covered by numerous big pores (2.9–10 μm in diameter). The porosity of the fiber inner surface was about 0.168 (pore area)/(total membrane area). So hollow fibers with a selective outer skin layer, a highly porous substructure, and a more open inner surface were formed under these spinning conditions.

The UF performance of these fibers was evaluated by feeding test solutions through the fiber bore and to its shell side. Experimental results showed that these hollow fiber membranes indeed possess a low transmembrane resistance. A full report on these performance results will be presented in a separate paper.

CONCLUSIONS

The polymer demixing rate at the fiber bore surface is influenced by the conditions of the internal coagulant, such as its viscosity, flow rate, and coagulation power. The most influential factor appears to be the coagulation power of the internal coagulant measured by the difference $\Delta\delta$ between the solubility parameter of the internal coagulant and that of the polymer. At high $\Delta\delta$ (>20 $MPa^{0.5}$), polymer precipitation rate is high and thus a dense skin layer is formed on the fiber inner surface. When $\Delta\delta$ is low (<4.1 $MPa^{0.5}$), the polymer at the fiber bore surface cannot precipitate but tends to dissolve into the internal coagulant. A very open fiber inner surface is thus formed at this low $\Delta\delta$, which helps lower the total transmembrane resistance.

REFERENCES

1. F. W. Altena, "Phase Separation Phenomena in Cellulose Acetate Solutions in Relation to Asymmetric Membrane Formation," Ph.D. Thesis, University of Twente, Enschede, 1982.
2. M. H. V. Mulder, J. O. Hendrikman, J. G. Wijmans, and C. A. Smolders, "A Rationale for the Preparation of Asymmetric Pervaporation Membranes," *J. Appl. Polym. Sci.*, *30*, 2805 (1985).
3. (a) A. J. Reuvers, J. W. A. van de Berg, and C. A. Smolders, "Formation of Membranes by Means of Immersion Precipitation. I. A Model to Describe Mass Transfer during Immersion Precipitation," *J. Membr. Sci.*, *34*, 45 (1987). (b) A. J. Reuvers and C. A. Smolders, "Formation of Membranes by Means of Immersion Precipitation. II. The Mechanism of Formation of Membranes Prepared from the System Cellulose Acetate–Acetone–Water, *Ibid.*, *34*, 67 (1987). (c) A. J. Reuvers, "Membrane Formation: Diffusion Induced Demixing Processes in Jernary Polymeric Systems," Ph.D. Thesis, University of Twente, Enschede, 1987.
4. (a) I. Cabasso, E. Klein, and J. K. Smith, "Polysulfone Hollow Fibers. I. Spinning and Properties, *J. Appl. Polym. Sci.*, *20*, 2377 (1970). (b) Cabasso, E. Klein and J. K. Smith, "Polysulfone Hollow Fibers. II. Morphology, *Ibid.*, *21*, 165 (1970).

5. J. G. Wijmans, J. Kant, M. H. V. Mulder, and C. A. Smolders, "Phase Separation Phenomena in Solutions of Polysulfone in Mixtures of a Solvent and a Nonsolvent: Relationship with Membrane Formation," *Polymer*, *26*, 1539 (1985).
6. J. G. Wijmans, J. P. B. Baaij, and C. A. Smolders, "The Mechanism of Formation of Microporous or Skinned Membranes Produced by Immersion Precipitation," *J. Membr. Sci.*, *14*, 263 (1983).
7. (a) J. A. van't Hof, A. J. Reuvers, R. M. Boom, H. H. M. Rolevink, and C. A. Smolders, "Preparation of Asymmetric Gas Separation Membranes with High Selectivity by a Dual-Bath Coagulation Method," *Ibid.*, *70*, 17 (1992). (b) J. A. van't Hof, "Wet Spinning of Asymmetric Hollow Fiber Membranes for Gas Separation," Ph.D. Thesis, University of Twente, Enschede, 1988.
8. H. D. W. Roesink, "Microfiltration: Membrane Development and Module Design," Ph.D. Thesis, University of Twente, Enschede, 1989.
9. (a) R. M. Boom, Th. van den Boomgaard, and C. A. Smolders, "Equilibrium Thermodynamics of a Quaternary Membrane Forming System with Two Polymers. I. Calculations, *Macromolecules*, *27*, 2034 (1994). (b) R. M. Boom, H. W. Reinders, H. H. W. Rolevink, U. Cordilia, Th. van den Boomgaard, and C. A. Smolders, "Equilibrium Thermodynamics of a Quaternary Membrane Forming System with Two Polymers. II. Experiments, *Ibid.*, *27*, 2041 (1994). (c) R. M. Boom, Th. van den Boomgaard, and C. A. Smolders, "Mass Transfer and Thermodynamics During Immersion Precipitation for a Two Polymer System: Evaluation with the System PES–PVP–NMP–Water, *J. Membr. Sci.*, *90*, 231 (1994). (d) R. M. Boom, "Membranes Formation by Immersion Precipitation: The Role of a Polymeric Additive," Ph.D. Thesis, University of Twente, Enschede, 1993.
10. (a) I. M. Wienk, H. A. Teunis, Th. van. den. Boomgaard, and C. A. Smolders, "A New Spinning Technique for Hollow Fiber Ultrafiltration Membranes," *J. Membr. Sci.*, *78*, 93 (1993). (b) I. M. Wienk, Th. van. den. Boomgaard, and C. A. Smolders, "The Formation of Nodular Structure in the Top Layer of Ultrafiltration Membranes," *J. Appl. Polym. Sci.*, *53*, 1011 (1994). (c) I. M. Wienk, "Ultrafiltration Membranes from a Polymer Blend-Hollow Fiber Preparation and Characterization," Ph.D. Thesis, University of Twente, Enschede, 1994.
11. (a) P. Radovanovic, S. W. Thiel, and S. T. Hwang, "Formation of Asymmetric Polysulfone Membranes by Immersion Precipitation. Part I: Modeling Mass Transport during Gelation," *J. Membr. Sci.*, *65*, 213 (1992). (b) P. Radovanovic, S. W. Thiel, and S. T. Hwang, "Formation of Asymmetric Polysulfone Membranes by Immersion Precipitation. Part II: The Effects of Casting Solution and Gelation Bath Composition on Membrane Structure and Skin Formation," *Ibid.*, *65*, 231 (1992).
12. J. H. Hilderbrand and R. L. Scott, *The Solubility of Non-Electrolytes*, Dover, New York, NY, 1964.
13. R. E. Kesting, *Synthetic Polymeric Membranes*, 2nd ed., Wiley, New York, NY, 1985.
14. A. F. M. Barton, *Handbook of Polymer–Liquid Interaction Parameters and Solubility Parameters*, CRC Press, Boca Raton, FL, 1990.
15. A. F. M. Barton, *Handbook of Solubility Parameters and Other Cohesion Parameters*, 2nd ed., CRC Press, Boca Raton, FL, 1991.
16. K. X. Ma, S. Sourirajan, H. Zhang, and W. W. Y. Lau, "Standardization in the Production and Testing Procedures for Polyethersulfone Hollow Fiber Ultrafiltration Membranes," *Sep. Sci. Technol.*, *30*, 3025 (1995).
17. F. W. Billmeyer Jr., *Textbook of Polymer Science*, 2nd ed., Wiley, New York, NY, 1971.

18. H. Wood, J. Wang, and S. Sourirajan, "The Effect of Polyethersulfone Concentration on Flat and Hollow Fiber Membrane Performance," *Sep. Sci. Technol., 28,* 2297 (1993).
19. W. W. Y. Lau, M. D. Guiver, and T. Matsuura, "Phase Separation in Carboxylated Polysulfone/Solvent/Water Systems," *J. Appl. Polym. Sci., 42,* 3215 (1991).
20. S. Doi and K. Hamanaka, "Pore Size Control Technique in the Spinning of Polysulfone Hollow Fiber Ultrafiltration Membranes," *Desalination, 80,* 167 (1991).
21. H. Strathmann, K. Koch, P. Amar, and R. W. Baker, "The Formation Mechanism of Asymmetric Membranes," *Ibid., 16,* 179 (1975).

Received by editor December 20, 1996
Revision received May 1997